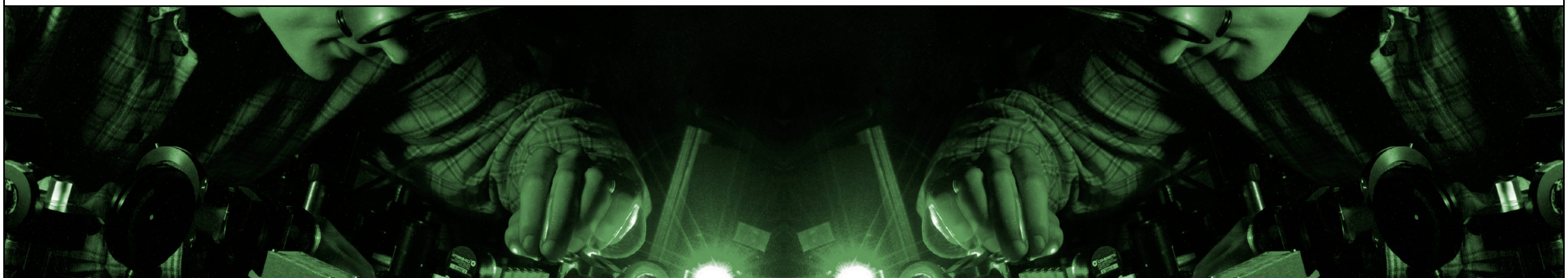

August 30, 2012

Optical Communication through Atmospheric Turbulence: Classical and Quantum

Jeffrey H. Shapiro

Optical and Quantum Communications Group

RESEARCH LABORATORY OF ELECTRONICS
Massachusetts Institute of Technology

www.rle.mit.edu/qoptics

Optical Communication through Atmospheric Turbulence: Classical and Quantum

- Refractive-index fluctuations and propagation phenomena
  - Kolmogorov inertial-subrange spatial spectrum and Taylor's hypothesis
  - beam spread, angle-of-arrival spread, multipath spread, and Doppler spread
- Extended Huygens-Fresnel principle
  - classical behavior: mutual coherence function and scintillation
  - propagation model for nonclassical light
- Classical communication: earth-space systems
  - diffraction-limited transmission
  - photon-bucket downlinks and adaptive-optics uplinks
- Turbulence effects on Bennett-Brassard 1984 quantum key distribution
  - near-field operation over terrestrial paths
  - far-field operation for airborne or satellite links

Temperature Fluctuations Create Refractive-Index Fluctuations

- Temperature fluctuations: $\Delta T \sim 1\,\mathrm{K}$
- Refractive-index fluctuations: $\Delta n \sim 10^{-6}$

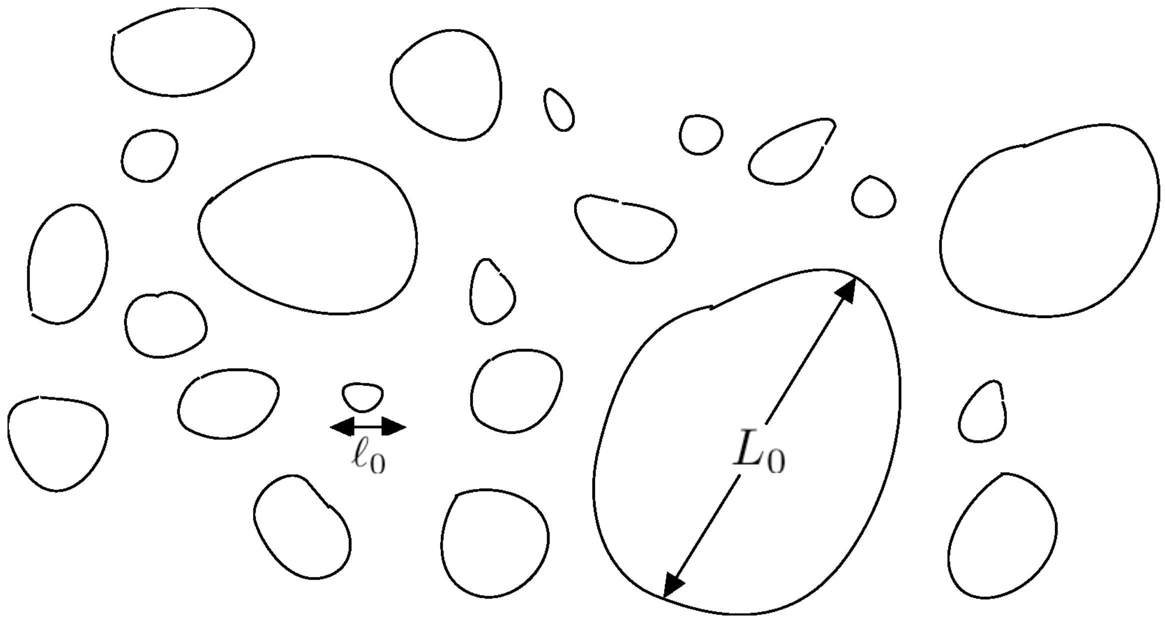

- Largest eddies: outer scale of turbulence L_0
- Smallest eddies: inner scale of turbulence ℓ_0
- Time dependence: eddy drift dominates eddy evolution

Refractive-Index Statistics: Kolmogorov Inertial-Subrange Turbulence

- Refractive-index structure function

$$
\begin{aligned}
D_{nn}(\mathbf{r}) &\equiv \langle [n(\mathbf{r}_o + \mathbf{r}) - n(\mathbf{r}_o)]^2 \rangle \\
&= C_n^2 |\mathbf{r}|^{2/3}, \text{ for } \ell_o \ll |\mathbf{r}| \ll L_o
\end{aligned}
$$

- Spatial spectrum

$$
\Phi_{nn}(\mathbf{K}) = 0.033\, C_n^2 |\mathbf{K}|^{-11/3}, \text{ for } 2\pi/L_o \ll |\mathbf{K}| \ll 2\pi/\ell_o
$$

- Refractive-index structure constant C_n^2
  - weak turbulence: $C_n^2 \sim 10^{-15}\,\mathrm{m}^{-2/3}$
  - strong turbulence: $C_n^2 \sim 10^{-12}\,\mathrm{m}^{-2/3}$

Spatial Spectrum of Turbulence: Inertial-Subrange Model

- Modified von Karman spectrum: $K_m \equiv 2\pi/\ell_o,\ K_o \equiv 2\pi/L_o$

$$\Phi_{nn}(\mathbf{K}) = \frac{0.033\, C_n^2 \exp[-(|\mathbf{K}|/K_m)^2]}{(K_o^2 + |\mathbf{K}|^2)^{11/6}}$$

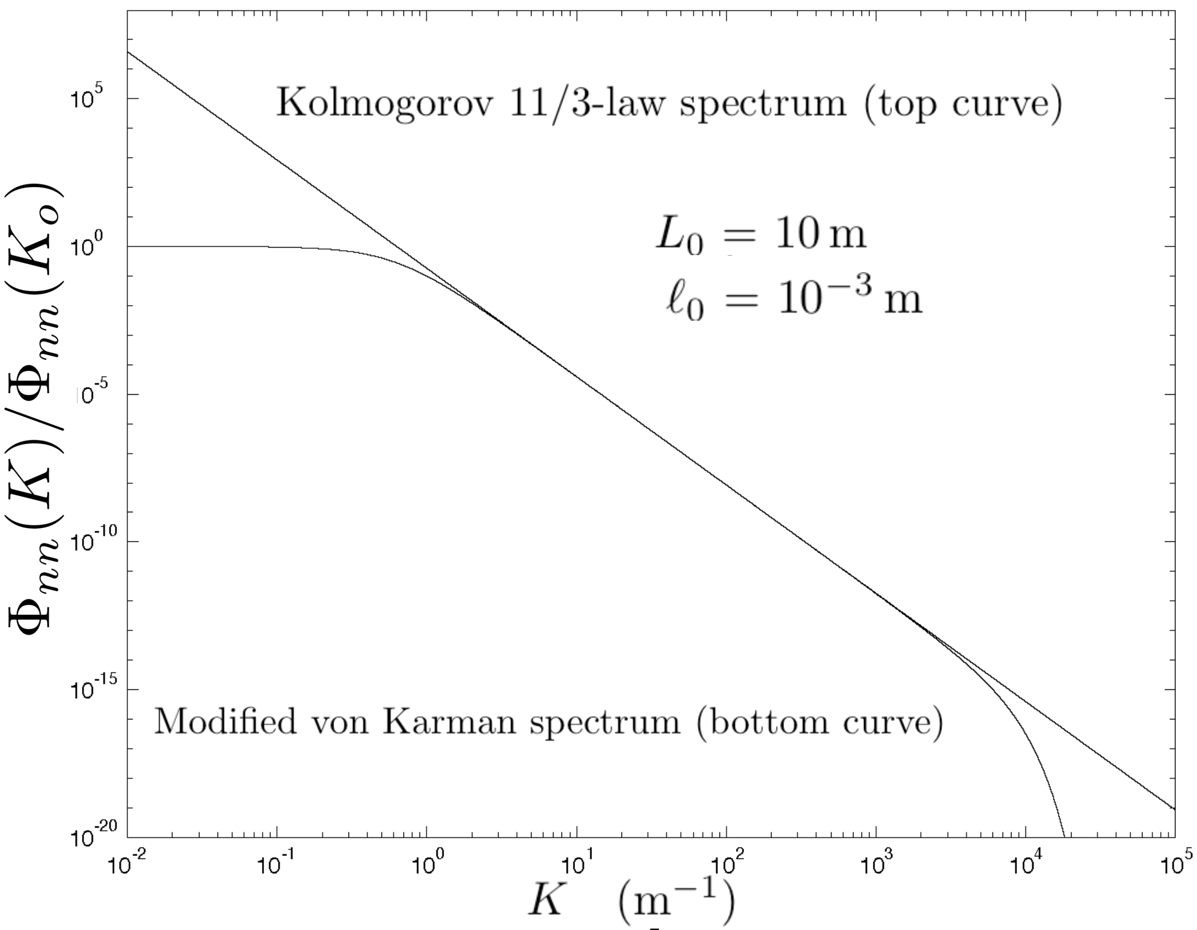

Line-of-Sight Propagation Phenomena: Spatial Effects

- Attenuation and depolarization
- Beam spread and angle-of-arrival spread

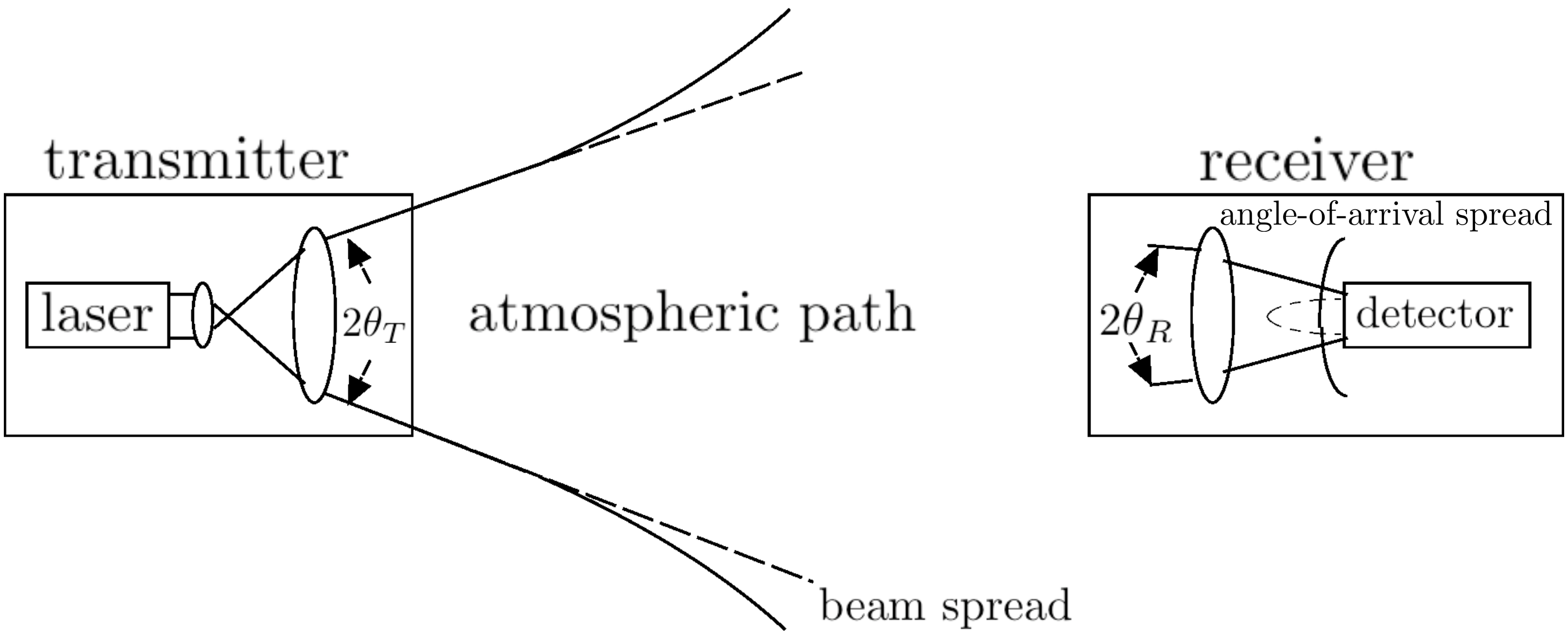

Line-of-Sight Propagation Phenomena: Temporal Effects

- Multipath spread
  - leads to intersymbol interference
- Doppler spread
  - leads to time-dependent fading

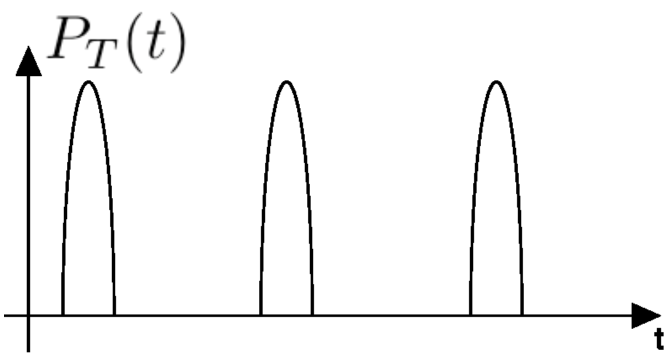

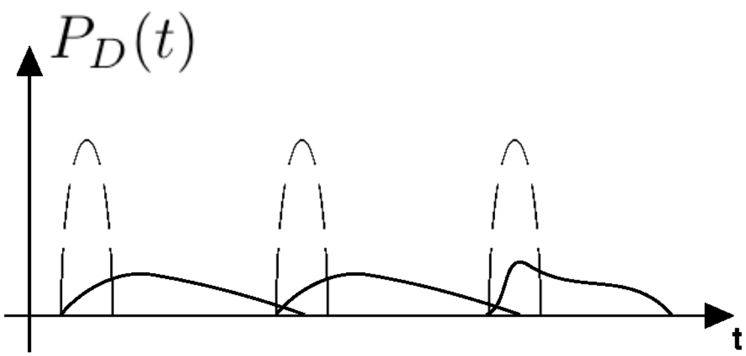

Optical Propagation through Turbulence

- Refractive-index fluctuations
  - real valued, isotropic, $\lambda \ll \ell_0$
- Clear-weather attenuation
  - atmospheric extinction over L -m-long path: $\exp(-\alpha L)$
- No depolarization
- Small scattering angles
  - beam spread and angular spread $\sim 10\,\mu\mathrm{R}$
  - multipath spread $< 1\,\mathrm{psec}$
- Wind-driven temporal effects
  - fade durations $\sim 1\text{–}10\,\mathrm{msec}$
  - Doppler spread $\sim 0.1\text{–}1\,\mathrm{kHz}$

Extended Huygens-Fresnel Principle: Classical Fields

- Input and output field envelopes: $E_0(\boldsymbol{\rho}, t)$ and $E_L(\boldsymbol{\rho}', t)$

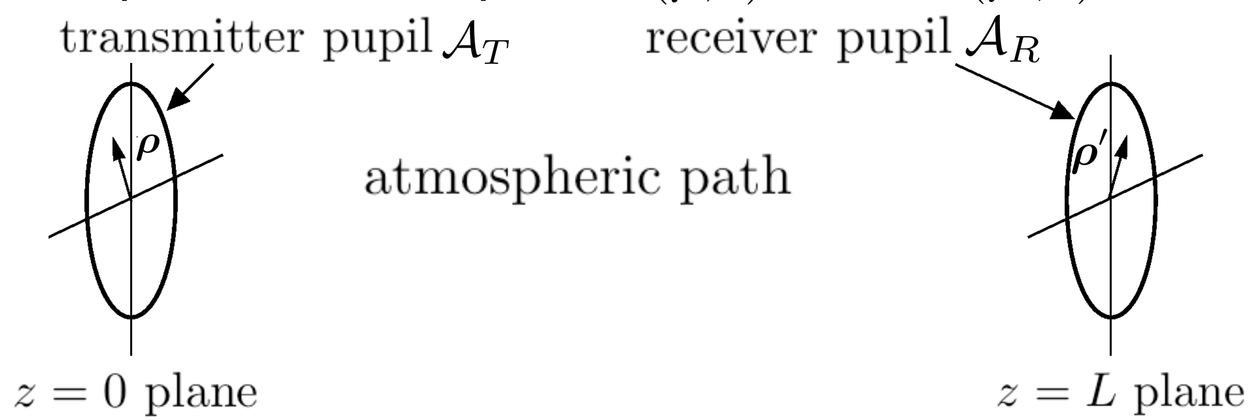

- Linear system input-output relation

$$E_L(\boldsymbol{\rho}', t) = \int_{\mathcal{A}_T} d\boldsymbol{\rho}\, E_0(\boldsymbol{\rho}, t - L/c) h(\boldsymbol{\rho}', \boldsymbol{\rho}, t)$$

- Atmospheric Green's function

$$h(\boldsymbol{\rho}', \boldsymbol{\rho}, t) = \frac{\exp[ik(L + |\boldsymbol{\rho}' - \boldsymbol{\rho}|^2/2L)]}{i\lambda L} \exp[\chi(\boldsymbol{\rho}', \boldsymbol{\rho}, t) + i\phi(\boldsymbol{\rho}', \boldsymbol{\rho}, t) - \overline{\alpha L}/2]$$

- Log-amplitude fluctuation: $\chi \longrightarrow$ scintillation
- Phase fluctuation: $\phi \longrightarrow$ beam spread and angle-of-arrival spread
- Attenuation: $\overline{\alpha L} \longrightarrow$ path-averaged atmospheric extinction

Extended Huygens-Fresnel Principle: Quantum Fields

- Input-plane and output-plane field operators: $\hat{E}_0(\boldsymbol{\rho}, t)$ and $\hat{E}_L(\boldsymbol{\rho}', t)$

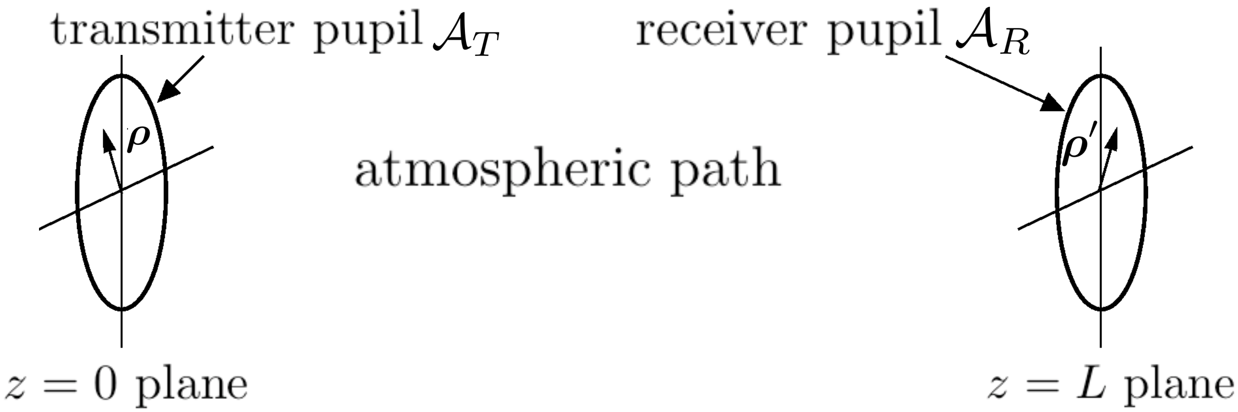

- Linear system input-output relation

$$\hat{E}_L(\boldsymbol{\rho}', t) = \int d\boldsymbol{\rho}\, \hat{E}_0(\boldsymbol{\rho}, t - L/c) h(\boldsymbol{\rho}', \boldsymbol{\rho}, t) + \sqrt{1 - e^{-\overline{\alpha L}}}\, \hat{E}_n(\boldsymbol{\rho}', t)$$

- Atmospheric Green's function same as for classical fields

$$h(\boldsymbol{\rho}', \boldsymbol{\rho}, t) = \frac{\exp[ik(L + |\boldsymbol{\rho}' - \boldsymbol{\rho}|^2/2L)]}{i\lambda L} \exp[\chi(\boldsymbol{\rho}', \boldsymbol{\rho}, t) + i\phi(\boldsymbol{\rho}', \boldsymbol{\rho}, t) - \overline{\alpha L}/2]$$

- Transmitter controls state of $\hat{E}_0(\boldsymbol{\rho}, t)$ inside $\mathcal{A}_T$
- Thermal-state background enters through $\hat{E}_0(\boldsymbol{\rho}, t)$ outside of $\mathcal{A}_T$
- Thermal-state background also enters through noise operator $\hat{E}_n(\boldsymbol{\rho}', t)$

Extended Huygens-Fresnel Principle: Fluctuation Statistics

- Mutual coherence function

$$\langle h^*(\boldsymbol{\rho}_1', \boldsymbol{\rho}_1, t) h(\boldsymbol{\rho}_2', \boldsymbol{\rho}_2, t) \rangle =$$

$$\frac{\exp[-ik(|\boldsymbol{\rho}_1' - \boldsymbol{\rho}_1|^2 - |\boldsymbol{\rho}_2' - \boldsymbol{\rho}_2|^2)/2L]}{(\lambda L)^2} \exp[-D(\boldsymbol{\rho}_1' - \boldsymbol{\rho}_2', \boldsymbol{\rho}_1 - \boldsymbol{\rho}_2)/2 - \overline{\alpha L}]$$

- Two-source spherical-wave wave structure function

$$D(\Delta\boldsymbol{\rho}', \Delta\boldsymbol{\rho}) = 2.91 k^2 \int_0^L dz\, C_n^2(z) |\Delta\boldsymbol{\rho}' z/L + \Delta\boldsymbol{\rho}(1 - z/L)|^{5/3}$$

- χ and ϕ often modeled as Gaussian processes*

- Temporal behavior via Taylor's hypothesis

*Gamma-gamma model is more appropriate for scintillation

Beam Spread and Angle-of-Arrival Spread

- Turbulence-limited beam divergence

$$\begin{aligned} \theta_T^o &= 0.384\lambda/\rho_o, \quad \text{half-angle} \\ \rho_o &\equiv \left(2.91k^2\int_0^L dz\, C_n^2(z)(1-z/L)^{5/3}\right)^{-3/5} \end{aligned}$$

  - turbulence near the transmitter dominates beam spread

- Turbulence-limited angle-of-arrival spectrum

$$\begin{aligned} \theta_R^o &= 0.384\lambda/\rho_o{}', \quad \text{half-angle} \\ \rho_o{}' &\equiv \left(2.91k^2\int_0^L dz\, C_n^2(z)(z/L)^{5/3}\right)^{-3/5} \end{aligned}$$

  - turbulence near the receiver dominates angle-of-arrival spread

- For C_n^2 = constant (horizontal path)

$$\begin{aligned} \rho_o = \rho_o{}' &= (1.09k^2C_n^2L)^{-3/5} \\ \theta_T^o = \theta_R^o &= \theta^o \end{aligned}$$

Scintillation: Log-Amplitude Variance

- Weak-perturbation regime
  - general case

$$\sigma_\chi^2 = 0.56k^{7/6}\int_0^L dz\, C_n^2(z)(L-z)^{5/6}(z/L)^{5/6}$$

    - mid-path turbulence dominates scintillation
  - for C_n^2 = constant (horizontal path)

$$\sigma_\chi^2 = 0.124k^{7/6}C_n^2L^{11/6}$$

  - scintillation correlation length $\sim \sqrt{\lambda L}$ (horizontal path)
- Strong-perturbation regime
  - saturation of scintillation: $\max(\sigma_\chi^2) \sim 0.3$
  - two-scale correlation:
    - short-scale $\sim \rho_o \ll \sqrt{\lambda L}$
    - long-scale $\gg \sqrt{\lambda L}$ (horizontal path)

Fade Depths for Lognormal Statistics

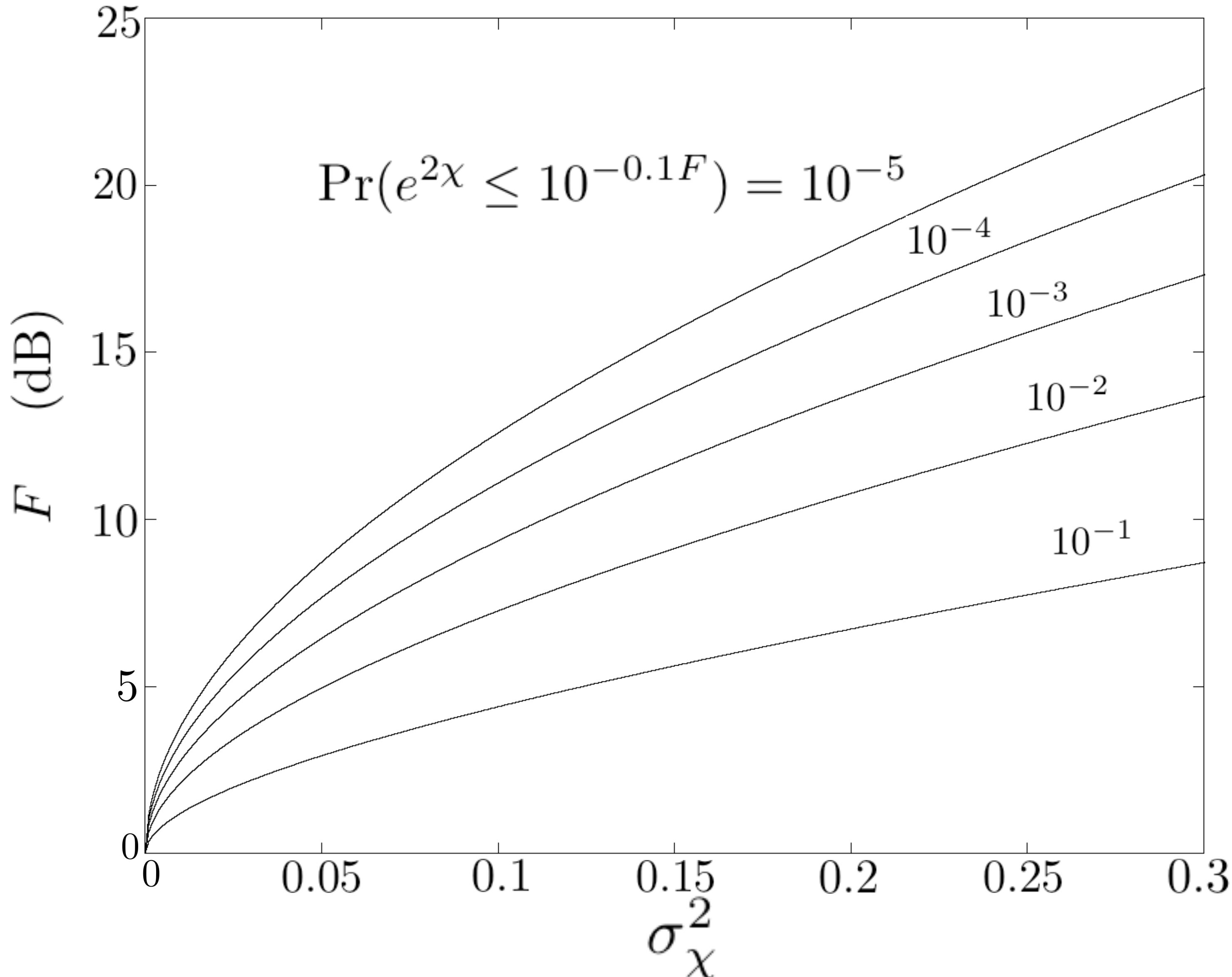

Aperture Averaging of Scintillation

- Large receivers average independent scintillations
  - gives reduced fading
- Aperture-integrated irradiance fluctuations
  - received power $P_R = \langle P_R \rangle e^{2u}$
  - aperture-integrated fade variable e^{2u} approximately lognormal
  - energy conservation $\rightarrow \langle u \rangle = -\sigma_u^2$
- Weak-perturbation regime aperture-averaging factor

$$e^{4\sigma_u^2} - 1 = \zeta \left(e^{4\sigma_\chi^2} - 1 \right)$$

$$\zeta \approx \frac{1}{1 + (d_R/\lambda L)^2}$$

Earth-Space Digital Communications

- Vacuum path much longer than atmospheric path

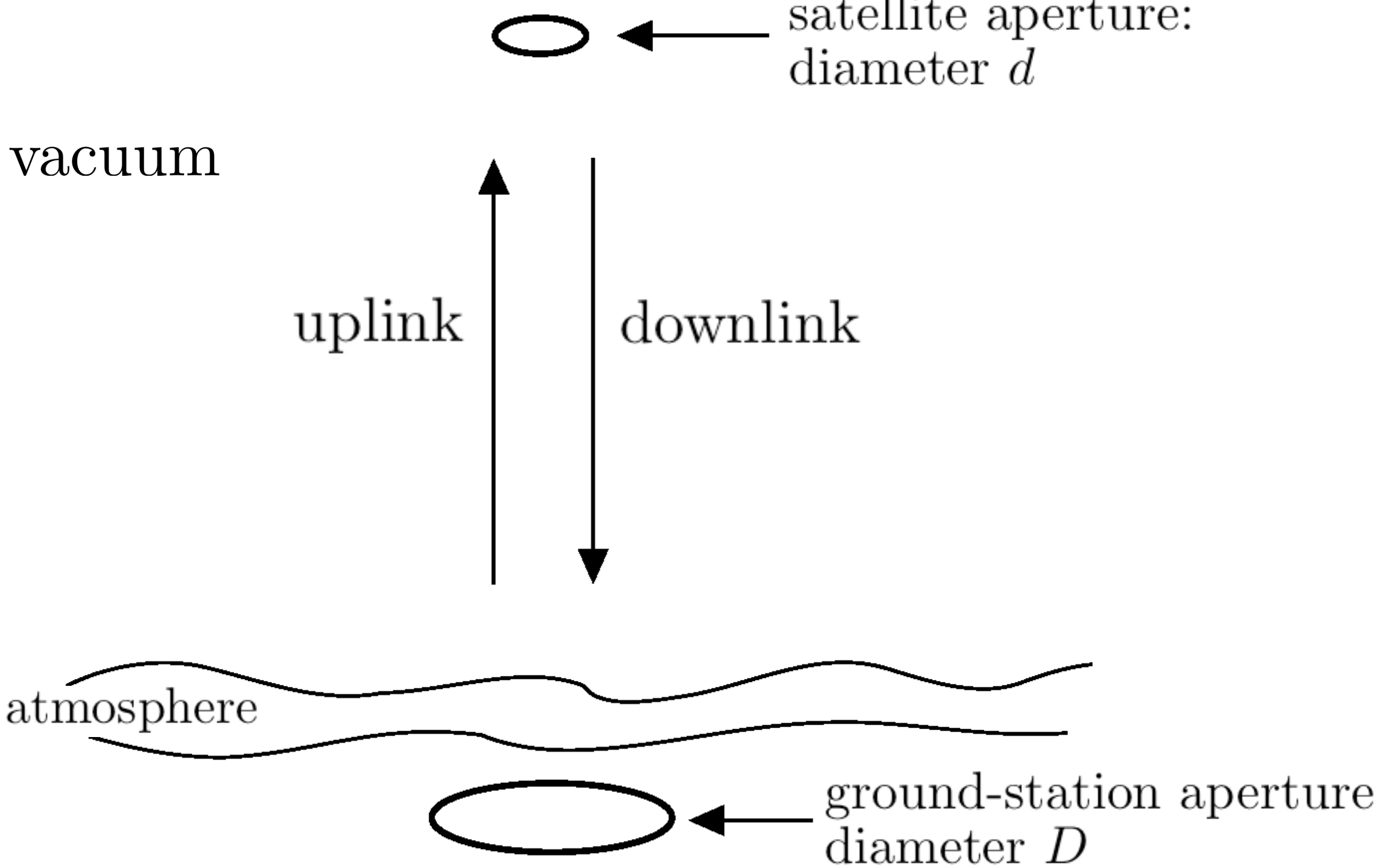

- Deep far-field operation: $D^2/\lambda L \ll 1, d^2/\lambda L \ll 1$
- Uplink suffers beam spread and fading
- Downlink suffers angle-of-arrival spread and fading

Bidirectional Earth-Space Communication: Binary Pulse-Position Modulation

- Collimated transmitters
- Multipath spread $\ll T \ll$ coherence time
  - flat fading with no dispersion
- Transmitted power waveforms: $m = 0, 1$

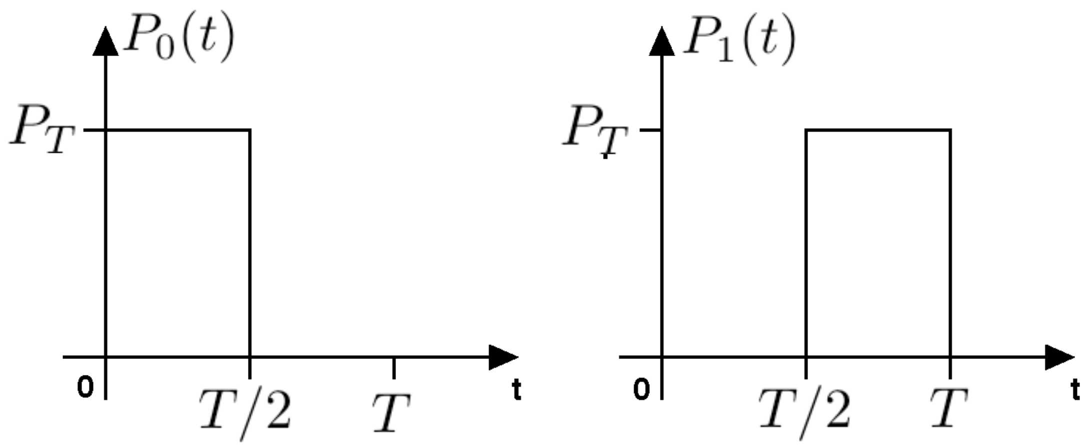

  - detected power waveforms are delayed and attenuated versions
- Vacuum-propagation case
  - diffraction-limited power transfer: $\dfrac{P_D}{P_T} = \left(\dfrac{\pi D d}{4\lambda L}\right)^2 \ll 1$

Turbulence-Limited Downlink Power Transfer: Diffraction-Limited Transmitter and Receiver

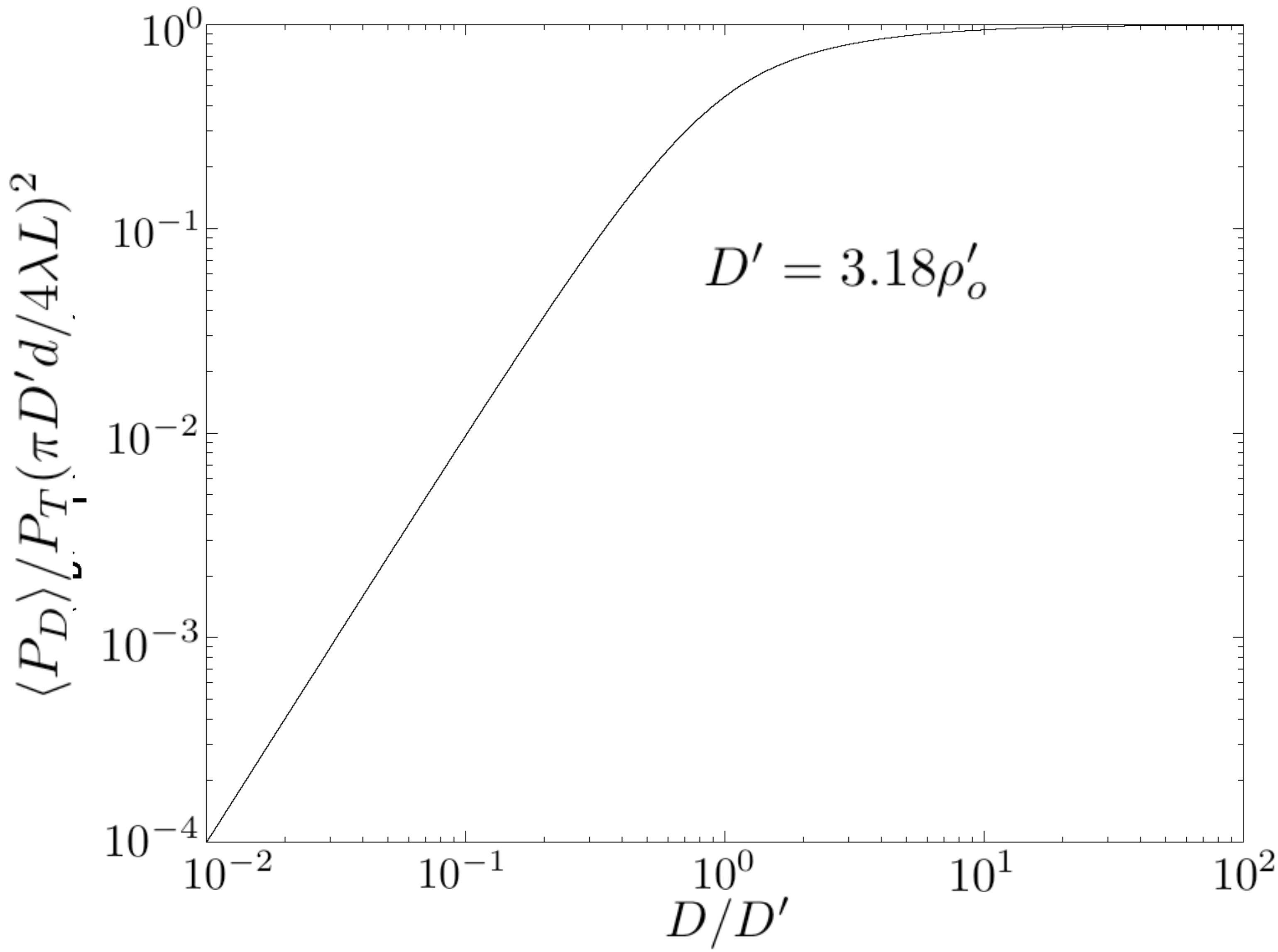

Direct-Detection Downlink Receivers: Diffraction-Limited versus Photon Bucket Operation

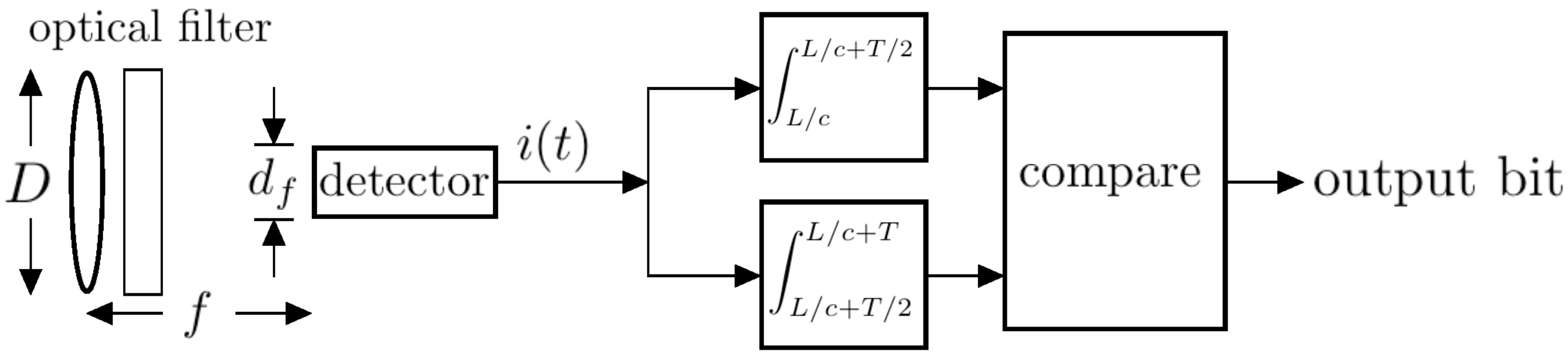

- Diffraction-limited receiver: $d_f \sim \lambda f/D$
  - Vacuum operation: optimum receiver
  - Atmospheric operation: suffers angle-of-arrival spread power loss
- Photon-bucket receiver: $d_f \sim \lambda f/\rho_0'$
  - atmospheric operation: collects all available signal power
  - collects much more than diffraction-limited background power

Shot-Noise-Limited Downlink Performance

- Vacuum-propagation diffraction-limited reception

$$\Pr(e) \le \begin{cases} 0.5\exp(-n_s), & \text{for } \mu \gg 1 \\ 0.5\exp(-n_s\mu/4), & \text{for } \mu \ll 1 \end{cases}$$

SNR threshold

- Atmospheric photon-bucket reception

$$\Pr(e) \le \begin{cases} 0.5\,\mathrm{Fr}(n_s, 0, \sigma_u), & \text{for } \mu \gg (D/D')^2 \\ 0.5\,\mathrm{Fr}(n_s\mu e^{4\sigma_u^2}(D'/2D)^2, 0, 2\sigma_u), & \text{for } \mu \ll (D/D')^2 \end{cases}$$

SNR fading threshold

- Signal, noise, and fading parameters
  - n_s = average number of detected signal photons
  - n_b = diffraction-limited detected background photons
  - $\mu \equiv n_s/n_b$ = diffraction-limited signal-to-background ratio
  - $D' = 3.18\rho_o'$ = turbulence limit on diffraction-limited performance
  - σ_u^2 = aperture-averaged log-amplitude variance

Lognormal-Density Error-Probability Integral

- $$\mathrm{Fr}(a,0,c) \equiv \int_0^\infty \mathrm{d}y\, \frac{\exp[-ay^2 - (\ln(y)+c^2)^2/2c^2]}{\sqrt{2\pi c^2}}$$

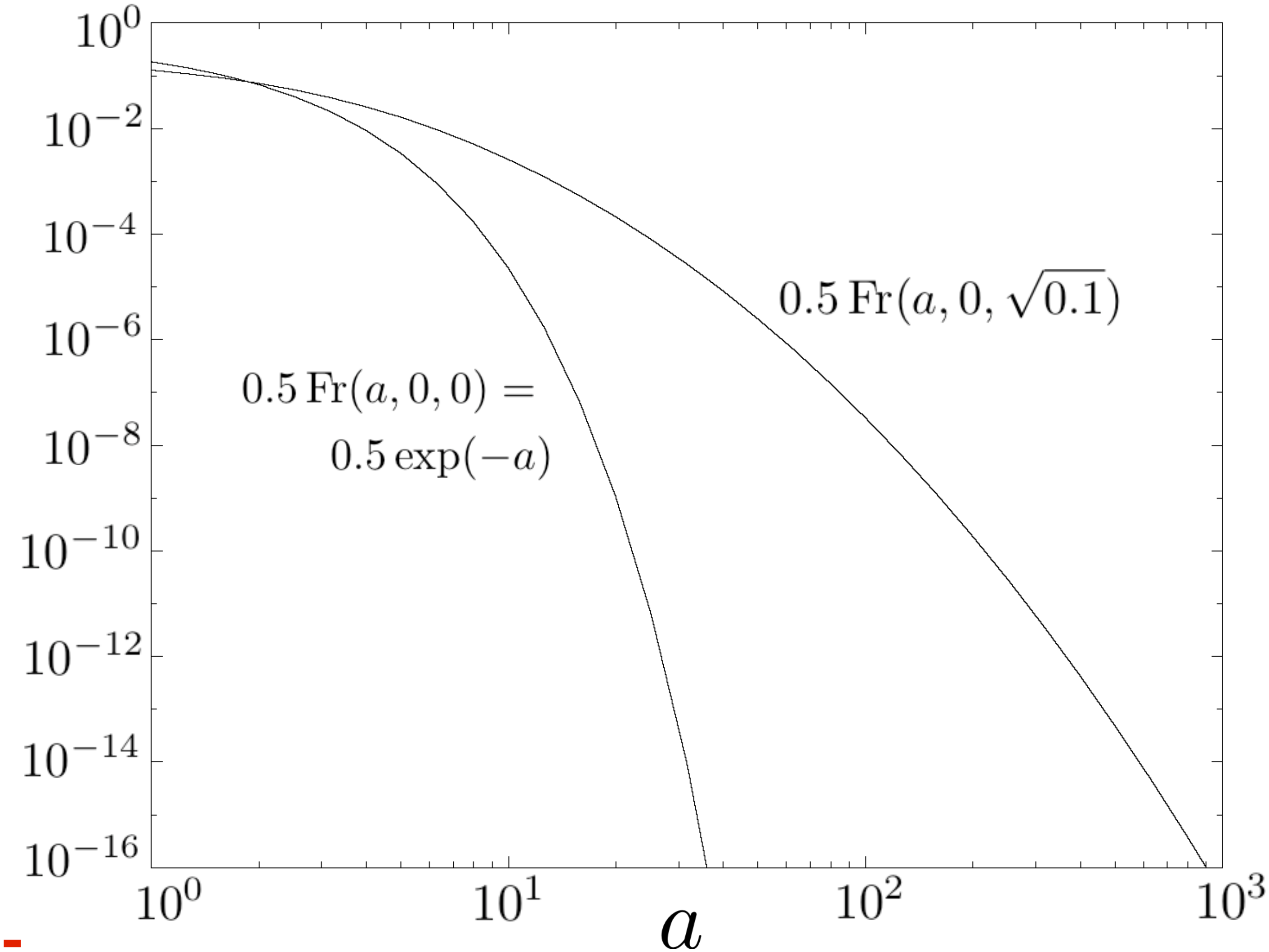

Phase-Compensated Downlink Reception

- Phase plate cancels turbulence phase
  - multiplies received field by $\exp[-i\phi(\boldsymbol{\rho}', \mathbf{0}, t)]$

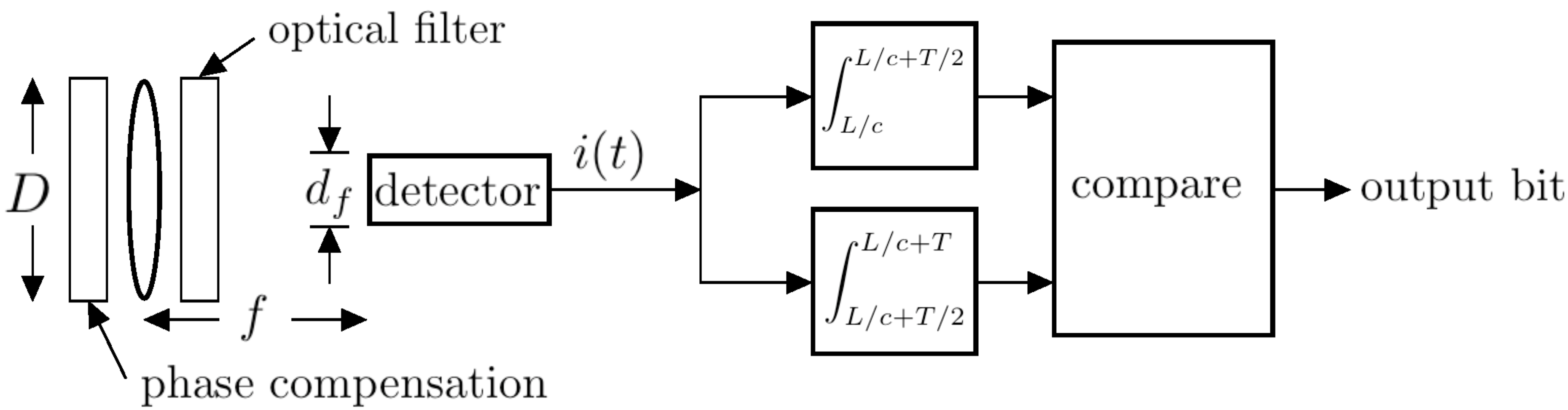

- Diffraction-limited performance: $d_f \sim \lambda f/D$

$$\Pr(e) \leq \begin{cases} 0.5\,\mathrm{Fr}(n_s e^{\sigma_u^2 - \sigma_\chi^2}, 0, \sigma_u), & \text{for } \mu \gg e^{\sigma_\chi^2 - \sigma_u^2} \\ 0.5\,\mathrm{Fr}(n_s \mu e^{6\sigma_u^2 - 2\sigma_\chi^2}/4, 0, 2\sigma_u), & \text{for } \mu \ll e^{\sigma_\chi^2 - \sigma_u^2} \end{cases}$$

Shot-Noise-Limited Uplink Performance

- Free-space diffraction-limited performance

$$\Pr(e) \le \begin{cases} 0.5\exp(-n_s), & \text{for } \mu \gg 1 \\ 0.5\exp(-n_s\mu/4), & \text{for } \mu \ll 1 \end{cases}$$

- Atmospheric diffraction-limited performance: $D \ll D'$

$$\Pr(e) \le \begin{cases} 0.5\,\mathrm{Fr}(n_s, 0, \sigma_\chi), & \text{for } \mu \gg 1 \\ 0.5\,\mathrm{Fr}(n_s\mu e^{4\sigma_\chi^2}, 0, 2\sigma_\chi), & \text{for } \mu \ll 1 \end{cases}$$

- No uplink version of downlink photon bucket
  - uplink beam spread cannot be dealt with incoherently

- Use uplink version of phase-compensated receiver

Extended Huygens-Fresnel Principle: Instantaneous Reciprocity: Earth-Space Path

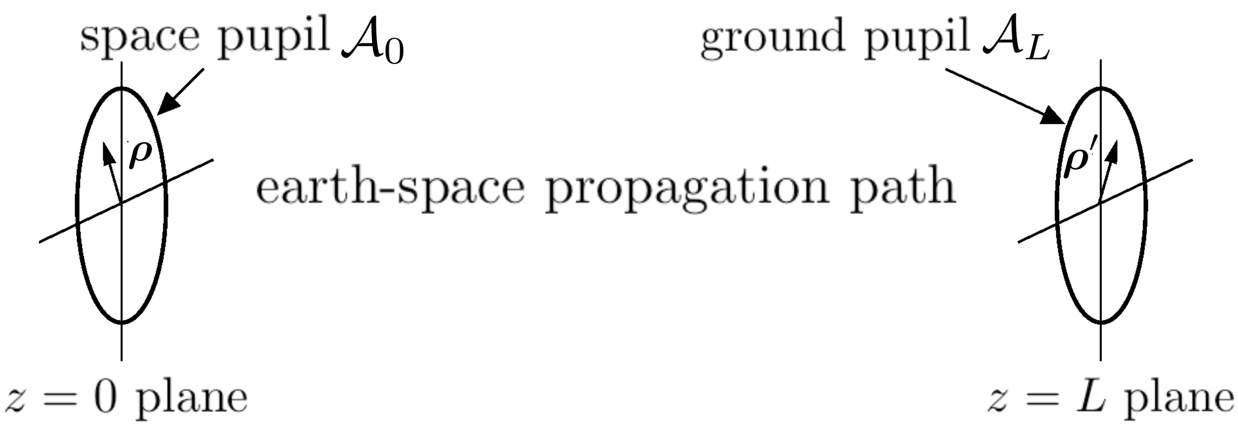

- $z = 0$ to $z = L$ propagation

$$E_L(\boldsymbol{\rho}', t) = \int_{\mathcal{A}_0} d\boldsymbol{\rho}\, E_0(\boldsymbol{\rho}, t - L/c) h(\boldsymbol{\rho}', \boldsymbol{\rho}, t)$$

- $z = L$ to $z = 0$ propagation

$$E_0(\boldsymbol{\rho}, t) = \int_{\mathcal{A}_L} d\boldsymbol{\rho}'\, E_L(\boldsymbol{\rho}', t - L/c) h(\boldsymbol{\rho}', \boldsymbol{\rho}, t - L/c)$$

Consequences of Atmospheric Reciprocity: Earth-Space Optical Communication

- Diffraction-limited downlink receiver: $D \ll D'$

$$\Pr(e) \le \begin{cases} 0.5\,\mathrm{Fr}(n_s, 0, \sigma_\chi), & \text{for } \mu \gg 1 \\ 0.5\,\mathrm{Fr}(n_s \mu e^{4\sigma_\chi^2}, 0, 2\sigma_\chi), & \text{for } \mu \ll 1 \end{cases}$$

  - same as diffraction-limited uplink transmitter

- Phase-compensated uplink transmitter: $D \gg D'$

$$\Pr(e) \le \begin{cases} 0.5\,\mathrm{Fr}(n_s e^{\sigma_u^2 - \sigma_\chi^2}, 0, \sigma_u), & \text{for } \mu \gg e^{\sigma_\chi^2 - \sigma_u^2} \\ 0.5\,\mathrm{Fr}(n_s \mu e^{6\sigma_u^2 - 2\sigma_\chi^2}/4, 0, 2\sigma_u), & \text{for } \mu \ll e^{\sigma_\chi^2 - \sigma_u^2} \end{cases}$$

  - same as photon-bucket downlink receiver

Bennett-Brassard 1984 Quantum Key Distribution

- Weak laser-source Alice without decoy states

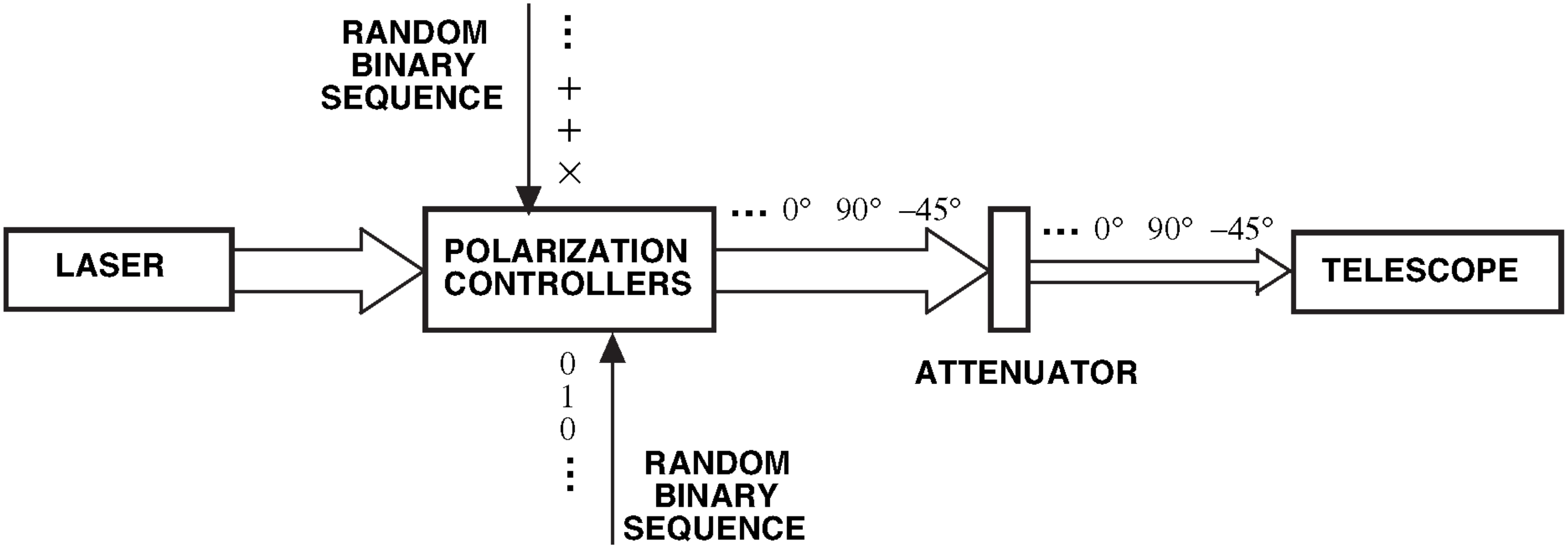

- Focused-beam spatial pattern

$$\xi_0(\boldsymbol{\rho}) = \sqrt{\frac{4}{\pi d^2}}\, \exp(-ik|\boldsymbol{\rho}|^2/2L), \ \text{for } |\boldsymbol{\rho}| \le d/2$$

Bennett-Brassard 1984 Quantum Key Distribution

- Passive basis-selection Bob with number-resolving detectors

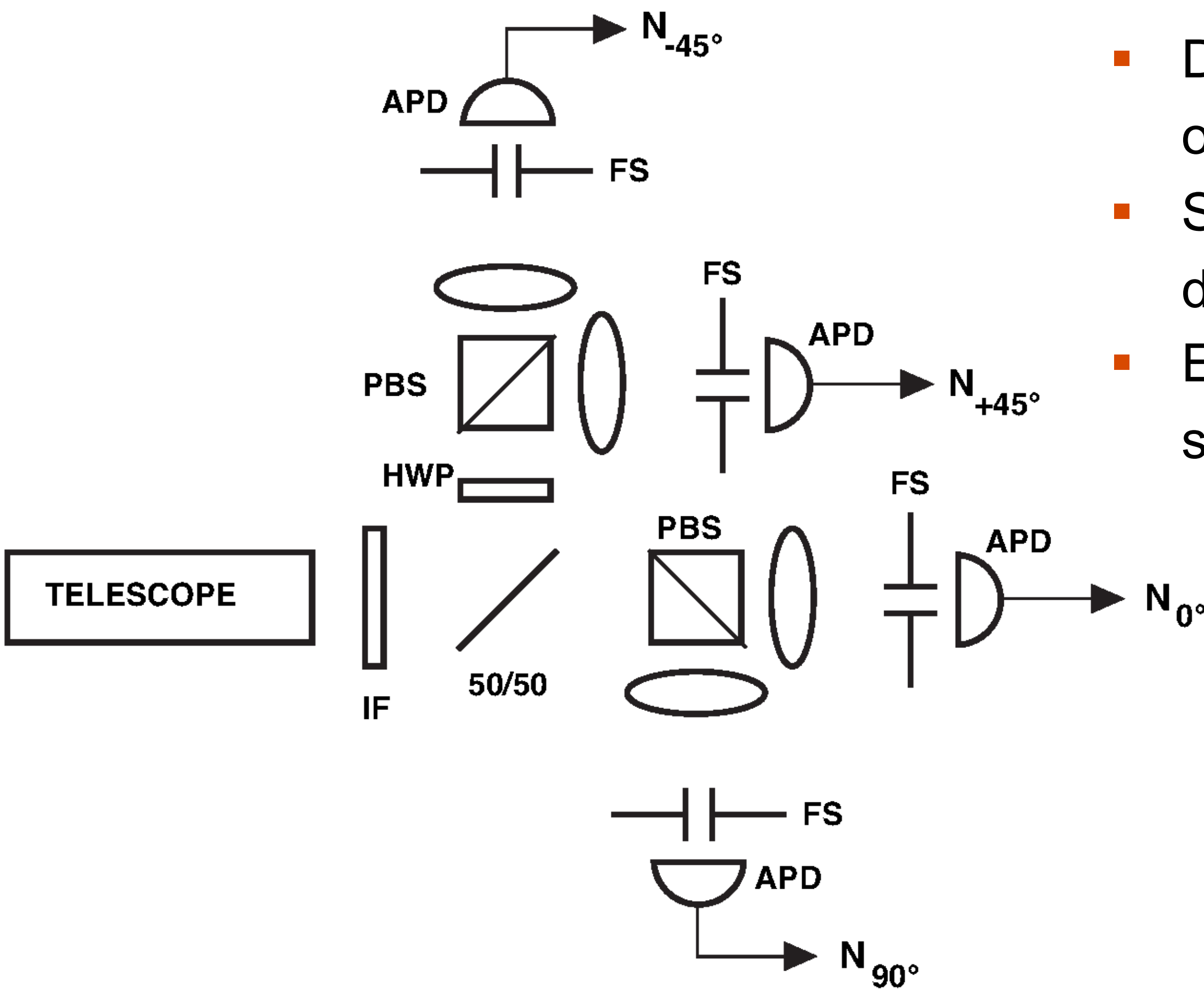

- Detection event:
  only one detector clicks
- Sift event:
  detection in Alice's basis
- Error event:
  sift with wrong polarization

Near-Field Terrestrial Operation

- Diameter d circular transmitter and receiver pupils
  - near-field power transfer regime: $(\pi d^2/4\lambda L)^2 \gg 1$

- System parameters

wavelength λ	$0.7\,\mu\text{m}$
average transmitted photon number n_S	0.5 or 1.0
path length L	$1\,\text{km}$
extinction coefficient α	$2\,\text{dB/km}$
turbulence strength C_n^2	$2 \times 10^{-14}\,\text{m}^{-2/3}$
turbulence coherence length ρ_0	$1.1\,\text{cm}$
logamplitude variance σ_χ^2	0.1
average background photon number n_B	10^{-3}
average dark-count number n_D	10^{-6}
detector quantum efficiency η	0.5

Near-Field Sift and Error Probabilities

- Sift probability

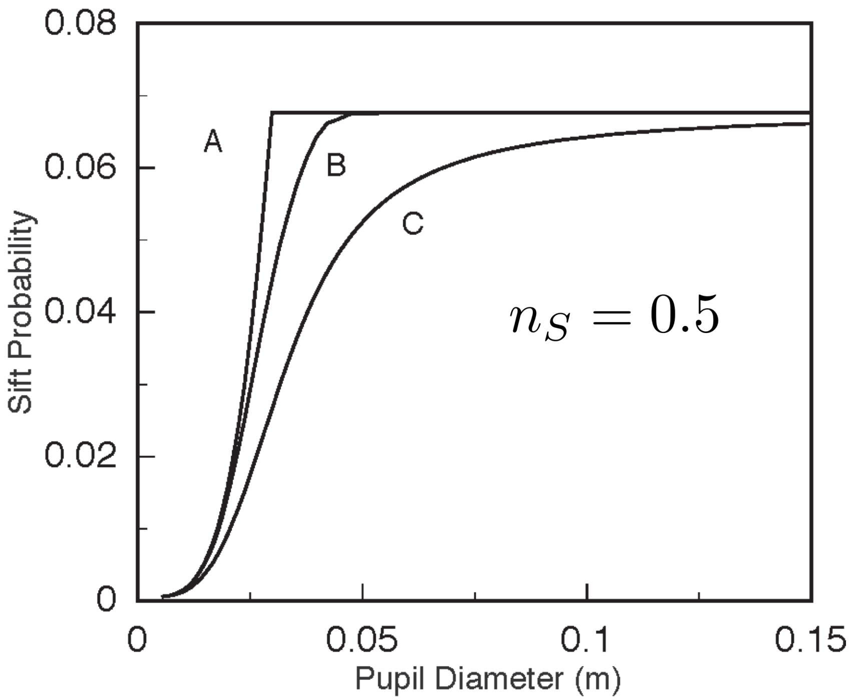

- A = turbulent-channel upper bound
- B = no-turbulence sift probability
- C = turbulent-channel lower bound

- Error probability

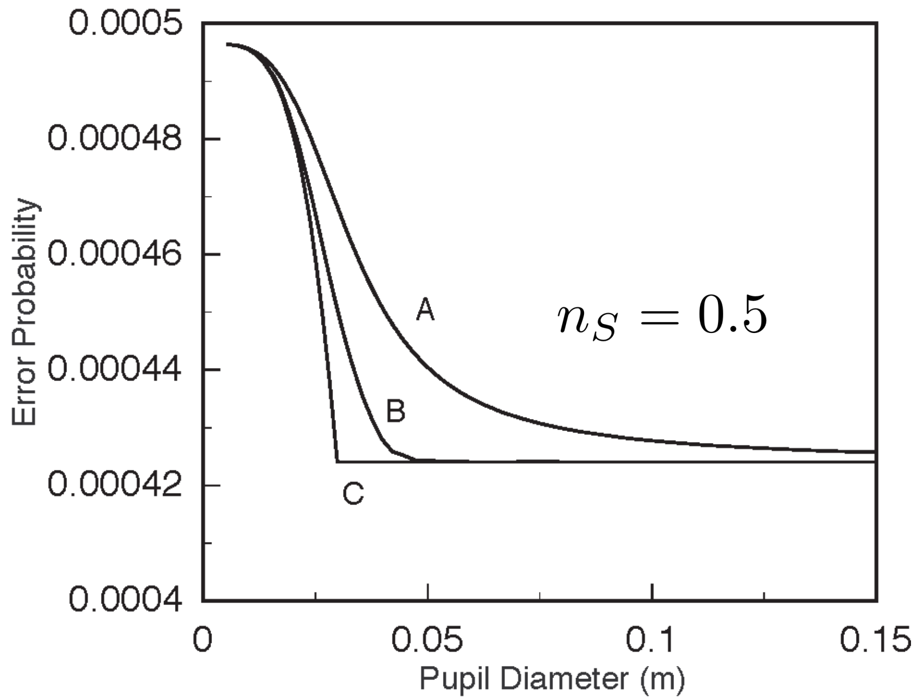

- A = turbulent-channel upper bound
- B = no-turbulence sift probability
- C = turbulent-channel lower bound

Shapiro, Phys. Rev. A **67**, 022309 (2003)

Near-Field Quantum Bit Error Rate (QBER)

- QBER = Pr(error|sift)

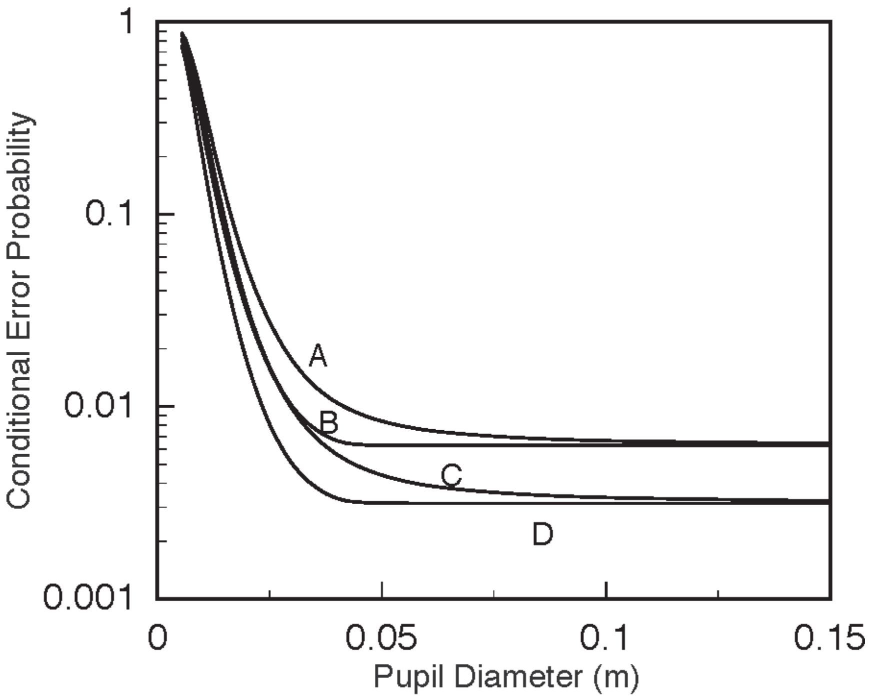

- For $d = 5.3$ cm and $n_S = 0.5$: QBER in turbulence *at most* 28% higher than no-turbulence case
- For $d = 5.3$ cm and $n_S = 1.0$: QBER in turbulence *at most* 39% higher than no-turbulence case

- A = turbulent-channel upper bound for $n_S = 0.5$
- B = no-turbulence QBER for $n_S = 0.5$
- C = turbulent-channel upper bound for $n_S = 1.0$
- D = no-turbulence QBER for $n_S = 1.0$

Shapiro, Phys. Rev. A **67**, 022309 (2003)

Far-Field Earth-Space Operation

- Circular transmitter and receiver pupils
  - diameter D_S in space, diameter D_G on the ground
  - far-field power transfer regime: $(\pi D_S D_G/4\lambda L)^2 \ll 1$
  - space pupil lies in single coherence area: no downlink beam spread
  - ground pupil has many coherence areas: uplink beam spread

- System parameters

average transmitted photon number n_S	0.5
no-turbulence fractional power transfer $\gamma_{\rm NT}$	10^{-3}
logamplitude variance σ_χ^2	0.5
aperture averaging factor ζ	1
average noise-photon number n_N	5×10^{-6}
detector quantum efficiency η	0.5

Far-Field Sift and Error Probabilities

- Downlink performance: Alice in space, Bob on ground

$$\left|\frac{\Pr(\text{sift})}{\Pr(\text{sift})_{\text{NT}}} - 1\right| = 1.52 \times 10^{-3} \quad \text{and} \quad \left|\frac{\Pr(\text{error})}{\Pr(\text{error})_{\text{NT}}} - 1\right| = 1.97 \times 10^{-7}$$

NT denotes no-turbulence

- Uplink performance: Alice on ground, Bob in space
  - collimated-beam transmitter: $\xi_0(\boldsymbol{\rho}) = \sqrt{4/\pi D_G^2}$, for $|\boldsymbol{\rho}| \leq D_G/2$

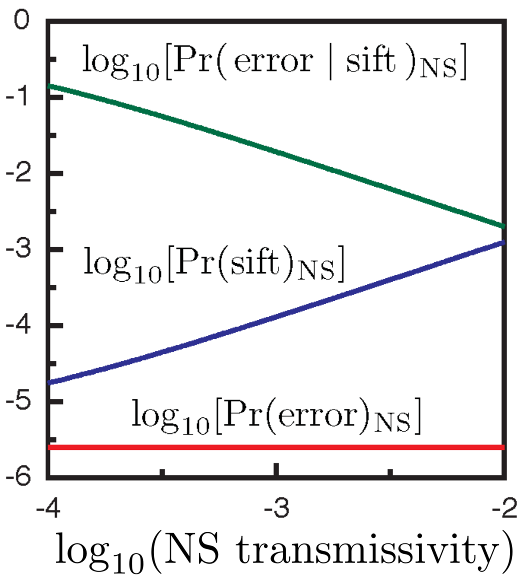

$$\max\left|\frac{\Pr(\text{sift})}{\Pr(\text{sift})_{\text{NS}}} - 1\right| = 2.48 \times 10^{-3}$$

$$\max\left|\frac{\Pr(\text{error})}{\Pr(\text{error})_{\text{NS}}} - 1\right| = 3.11 \times 10^{-6}$$

$$\max\left|\frac{\Pr(\text{ error} \mid \text{sift })}{\Pr(\text{ error} \mid \text{sift })_{\text{NS}}} - 1\right| = 2.49 \times 10^{-3}$$

Shapiro, Phys. Rev. A **84**, 032340 (2011)

NS denotes no-scintillation

Optical Communication through Atmospheric Turbulence: Classical and Quantum

- Refractive-Index Fluctuations
  - Universal correlation behavior in Kolmogorov inertial subrange
  - Temporal statistics via wind-driven shift of spatial statistics
- Line-of-Sight Propagation Phenomena
  - Extinction due to molecules and aerosols, no depolarization
  - Beam spread and angle-of-arrival spread $\sim 10\,\mu\mathrm{R}$
  - Multipath spread $< 1\,\mathrm{psec}$, Doppler spread $\sim 0.1\text{–}1\,\mathrm{kHz}$
- Extended Huygens-Fresnel Principle
  - Mutual coherence function behavior: two-source structure function
  - Scintillation behavior: long-lived deep fades
  - Quantum operators propagate like classical fields
- Classical communication and BB84 QKD
  - Turbulence-limited far-field power transfer for multi-coherence-area transmitters
  - Deep scintillation fades are major problem for classical communication
  - Scintillation has minimal impact on both near-field and far-field BB84 QKD